The Influence of Boundary Layer Pumping on Synoptic-Scale Flow

L. MAHRT AND SOON-UNG PARK

Department of Atmospheric Sciences, Oregon State University, Corvallis 97331

(Received 12 February 1976, in revised form 12 April 1976)

ABSTRACT

The influence of boundary layer pumping on an externally forced, synoptic-scale flow is examined. The results follow earlier theories of stratified incompressible Boussinesq flow theories in that the spin-down time scale and the penetration depth of the influence of boundary layer pumping are inversely proportional to the stratification and proportional to the horizontal length scale of the flow. The present development is performed in isentropic coordinates to construct estimates applicable to the atmosphere. This analysis indicates that boundary layer pumping could be synoptically important in the lower troposphere under conditions of significant surface stress and tropospheric stratification.

The estimate of the stratified penetration depth scale is used to construct a simple homogeneous model to examine order-of-Rossby-number corrections to the quasi-geostrophic vorticity dynamics. Such corrections result from the influence of accelerations in both the free flow and boundary layer. It is found, for example, that vorticity adjustments due to various interactions between boundary layer pumping and accelerations are less important than predicted by scale analyses. Results are interpreted for the case of topographically forced flow.

1. Introduction

Non-zero synoptic-scale geostrophic vorticity in the presence of low-level turbulent momentum transports, hereafter referred to as boundary layer or frictional effects, leads to low-level convergence or divergence and vertical motions (Charney and Eliassen, 1949). Such frictionally driven convergence is thought to contribute substantially to the maintenance of clouds and precipitation patterns (Petterssen, 1956, Sec. 5.7). However, in the absence of latent heating, this "frictionally driven" boundary layer "pumping" in turn acts to destroy the existing geostrophic relative vorticity in the overlying free flow through induced vortex stretching. The effects of such negative boundary layer feedback is illustrated in the intermediate stage of Ekman spin-down or spin-up theory (Greenspan and Howard, 1963; Holton, 1965). As long as the turbulent Ekman number is small, as is usually the case with atmospheric circulations, the above spin-down process is more efficient on a synoptic time scale than direct turbulent transport or diffusion of vorticity. Thus, boundary layer pumping is often considered to be an important interaction between the synoptic scale and turbulent scales of motion.

However, the interaction between synoptic-scale vorticity dynamics and boundary layer pumping is also complicated by accelerations, baroclinity and stratification, vertical fluxes of heat, latent heat release, latitudinal variations of the Coriolis parameter, as well as complications due to interactions with intermediate scales of motion such as internal gravity waves. For example, when latent heating is directly coupled to the boundary layer vertical motion field, the effect of boundary layer pumping may be quite different than in simple spin-down (Charney and Eliassen, 1964).

Presently, we focus on the role of accelerations and free-flow stratification in altering the character of effects due to boundary layer pumping. Stratification is generally important on synoptic scales in the atmosphere (Phillips, 1963). Only flows with relatively weak stratification and/or large horizontal length scale behave to a first approximation as a homogeneous fluid. An example of such flow is discussed by Ingersoll (1969). In flows where stratification is important, the intensity of circulations induced by boundary layer pumping decreases with height (Holton, 1965; Walin, 1969; Buzyna and Veronis, 1971). The flow above a certain "penetration" depth is only weakly affected by spin-down processes on a synoptic time scale. In the free flow below the penetration depth scale, where the mass flux out of the boundary layer is concentrated, the importance of boundary layer pumping and the spin-down rate is greater compared to the case of a homogeneous fluid. Results due to Buzyna and Veronis (1971) and Walin (1969) also suggest that the depth of penetration of circulations induced by boundary layer pumping increases with horizontal length scale of the flow. We assume the diffusion of vorticity in the free flow to be unimportant on a synoptic time scale and thus do not consider the final diffusive stage of

spin-down (Greenspan and Howard, 1963; Sakurai, 1969).

In Section 3, we address two aspects of stratified atmospheric flow: 1) When, if ever, is boundary layer pumping important in a synoptic-scale flow? 2) What is the penetration depth scale of boundary layer pumping on a synoptic time scale? The influence of synoptic-scale accelerations is neglected in this analysis, but considered in Sections 4–6.

Accelerations in the boundary layer modify the boundary layer pumping rate while free-flow accelerations alter the rate of free flow vortex stretching due to a given boundary layer pumping rate. Young (1973) and Mahrt (1974) demonstrate that the role of accelerations in the boundary layer of a barotropic atmosphere is primarily to reinforce free flow vertical motions. However, the qualitative influence of advective accelerations on convergence is distinctly altered by frictional effects (Mahrt, 1975). These studies indicate that synoptic-scale accelerations can alter cross-isobar flow and boundary layer pumping as much as typical variations of surface stress. At low latitudes, rapid latitudinal variations of the Coriolis parameter induce large accelerations which can completely change the influence of synoptic-scale boundary layer covergence (Holton, 1975).

In Sections 4–6, we modify the quasi-geostrophic vorticity dynamics examined in Ingersoll (1969) and Huppert and Stern (1974) to include the first-order corrections due to the influence of synoptic-scale accelerations in the free flow and the boundary layer. We choose the simplest possible model which contains such effects. For this portion of the study, the free flow is homogeneous, adiabatic, invariant in one horizontal direction, and characterized by constant Coriolis parameter. The boundary layer is parameterized in terms of a conventional pumping law but modified to include the influence of synoptic-scale accelerations. The appropriate depth of the homogeneous fluid is assigned from the stratified flow theory developed in Section 3. In this manner, the importance of mass fluxes due to boundary layer pumping relative to the free flow mass flux is reasonably approximated by the homogeneous model.

These studies of the influence of accelerations are applied to the case of a synoptically forced flow. Results are interpreted in terms of orographical forcing. On a synoptic scale, orographical forcing or boundary forcing induces divergence or vortex contraction which in turn forces vorticity adjustments. As an example, Hess and Wagner (1948), McClain (1960) and others have suggested that orographically forced vortex stretching may significantly contribute to, but by no means completely explain, the high frequency of cyclogenesis observed immediately downstream from major mountain ranges (Petterssen, 1956).

2. Boundary layer pumping

We assume that the boundary layer is sufficiently thin or that it is sufficiently well-mixed, so that we can neglect the influence of boundary layer stratification and baroclinity [considered by Kuo (1973)]. The vertical motion w_h at the top of the boundary layer can then be shown to be proportional to the relative geostrophic vorticity ζ_g at the top of the boundary layer in which case

$$w_h = F\zeta_g + \mathrm{Ro}w_1, \tag{1}$$

where $\mathrm{Ro}w_1$ is the contribution to the vertical motion at the top of the boundary layer due to accelerations in the boundary layer, to be estimated in Sections 4–6. Since for constant Coriolis parameter f, the difference between geostrophic and actual vorticity is $O(\mathrm{Ro}^2)$ as can be seen by expanding flow variables in terms of the Rossby number, we can also write

$$w_h = F\zeta + \mathrm{Ro}w_1 + O(\mathrm{Ro}^2). \tag{2}$$

Here F can be interpreted as the thickness required to produce vertical motion w_h in the hypothetical case, where the cross-isobar flow speed equals the geostrophic wind speed. In the case of Ekman flow with constant viscosity or eddy viscosity K (Charney and Eliassen, 1949),

$$F \approx (K/2f)^{\frac{1}{2}} \sin 2\alpha, \tag{3}$$

where α is the angle between the surface geostrophic and actual flows. In the case of a turbulent boundary layer approximated by use of a linearized drag law (e.g., Mahrt, 1974)

$$F \approx \hat{C}_D h/(1+\hat{C}_D{}^2), \quad \hat{C}_D \approx C_D U/fh, \tag{4}$$

where C_D is a surface drag coefficient, U a horizontal velocity scale or boundary layer geostrophic wind speed and h is the boundary layer depth. The use of a linearized drag law allows simple extension of the pumping law (2) to cases of non-zero accelerations. In quasi-geostrophic flow, errors resulting from such a linearization are small or comparable to errors associated with uncertainties in the surface drag coefficient. For synoptically interesting flows, for $f=10^{-4}$ s^{-1} and $h=10^3$ m, F can be expected to vary typically from 25 m for $C_D=10^{-3}$ and $U=2.5$ m s^{-1} to 400 m for $C_D=4\times10^{-3}$ and $U=10$ m s^{-1}. F may vary substantially less for boundary layers where mechanical production of turbulence is important in which case h and C_DU are negatively correlated. In the above two numerical examples, $\hat{C}_D$ varies from 0.025 to 0.3 in which case F is approximately C_DU/f. Eq. (3) for $K=10$ m^2 s^{-1} and $\alpha=15°$, yields $F\approx110$ m. At lower latitudes, F and thus the cross-isobar flow for a given geostrophic wind can be expected to be larger.

Entrainment at the boundary layer/free flow interface does not formally affect the dynamics of vorticity

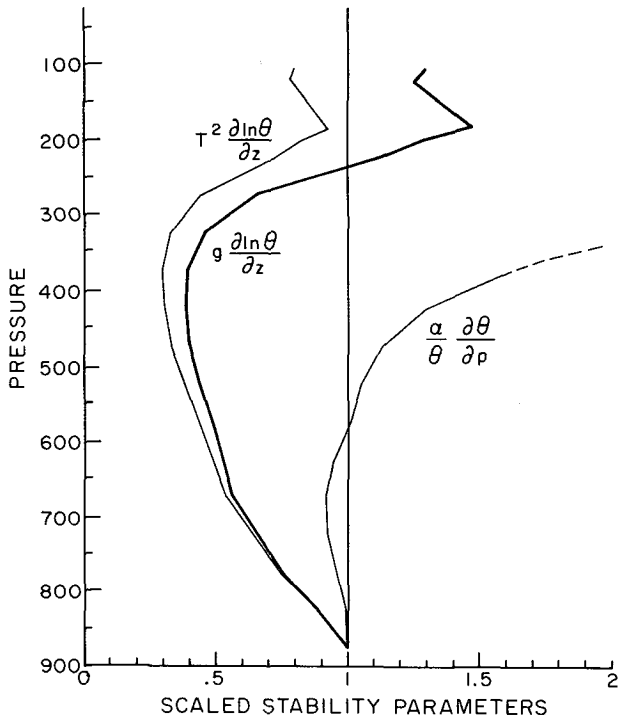

FIG. 1. Profiles of stability parameters for 50 mb layers from 900–200 mb and 25 mb layers for 200–100 mb. Layer stabilities are scaled with respect to values in lowest layer (900–850 mb). Profiles are averaged over the 38 U. S. radiosonde stations whose surface pressure remains below 900 mb. Each station profile is the average of 10 Januarys, 1946–55 [see Gates (1961) for analyses of additional stability parameters for slightly different data set].

adjustments due to boundary layer pumping, but merits brief consideration. In the case of zero entrainment, the boundary layer top is a substantial surface; no free flow is entrained into the boundary layer by turbulent actions at the boundary layer upper edge. In this case, the time rate of change of boundary layer depth is equal to the synoptic-scale vertical motion. In the other limiting case, the depth of the boundary layer remains fixed. In this hypothetical case, subsidence is compensated by entrainment of nonturbulent fluid into the boundary layer while rising motion implies destruction of turbulence energy by dissipation or buoyancy effects. In this limiting case, the boundary layer acts as a sink or source of nonturbulent fluid. The atmospheric boundary layer is generally not well approximated by either of the above limiting cases since both entrainment processes and depth changes are generally important. Not wishing to include an additional equation for entrainment rate (e.g., Lilly, 1968), we interpret subsequent results by viewing the boundary layer top to be a substantial surface.

3. Stratified theory

To estimate the depth and time scales describing the influence of boundary layer pumping as well as its importance in the stratified atmosphere on a synoptic time scale, we derive the adiabatic quasi-geostrophic "potential vorticity equation" in isentropic coordinates. We then perform an analysis mathematically quite similar to that of Walin (1969) and Buzyna and Veronis (1971) who analyzed spin-down of a stratified, incompressible, Boussinesq flow in Cartesian coordinates.

By using pressure, log-pressure or isentropic coordinates, a Boussinesq-type linearization of the pressure gradient term is not needed. However, approximate solutions in isentropic coordinates still require a Boussinesq-type approximation to the continuity equation while developments in log-pressure coordinates require simplification of an extra nonlinear stability-divergence term in the final potential vorticity equation.

A stability parameter appears as the coefficient of the second-order vertical derivative of the streamfunction tendency in the potential vorticity equation of each coordinate system. This stability parameter must be assumed constant for convenient analytical treatment. The stability parameters resulting from developments in pressure coordinates, $(\partial\phi/\partial p)(\partial \ln\theta/\partial p)$ [e.g., Haltiner, 1971, p. 154], in log-pressure coordinates, $\sim T^2\,(\partial \ln\theta/\partial z)$ [e.g., Phillips, 1963], and in isentropic coordinates, $g(\partial \ln\theta/\partial z)$, are estimated from January radiosonde data averaged over 10 years (U. S. Weather Bureau, 1957) and 38 U. S. stations in a manner similar to the analyses of Gates (1961). The mean vertical variations of such stability parameters are shown in Fig. 1. The stability parameter in isentropic coordinates is slightly less variable in the troposphere while the stability parameter in log-pressure coordinates is least variable for the troposphere and stratosphere as a whole. However, the stratosphere is presently not of concern since the important direct influence of boundary layer pumping on a synoptic time scale appears to be limited to the lower troposphere as will be discussed in Section 3c. The stability parameter for pressure coordinates is quite variable (see also Gates, 1961).

Examination of adiabatic flow in isentropic coordinates implicitly includes vertical advections and vorticity changes due to tilting terms. Such terms are normally neglected and do not appear even as first-order corrections in quasi-geostrophic developments where the basic state is geostrophic. However, immediately above the boundary layer, they may be substantially larger than predicted by scale analyses. At this level, vertical motions and vertical gradients are expected to be a maximum as a result of exponential-like decay with height of spin-down influences (Walin, 1969; Buzyna and Veronis, 1971). Based on the above considerations, we find isentropic coordinates slightly preferable. However, the choice of the coordinate system does not seem to influence the qualitative behavior of the flow solution.

a. Equations in isentropic coordinates

The governing equations in isentropic coordinates for frictionless adiabatic hydrostatic flow (e.g., Thompson, 1961) are

$$\partial u/\partial t+u\partial u/\partial x+v\partial u/\partial y-fv=-\partial M/\partial x, \tag{5}$$

$$\partial v/\partial t+u\partial v/\partial x+v\partial v/\partial y+fu=-\partial M/\partial y, \tag{6}$$

$$\partial M/\partial\theta=c_pT/\theta, \tag{7}$$

$$M\equiv c_pT+gZ, \tag{8}$$

$$\theta\equiv T(p_0/p)^{\kappa}, \tag{9}$$

$$\frac{\partial}{\partial t}\left(\frac{\partial p}{\partial\theta}\right)+u\frac{\partial}{\partial x}\left(\frac{\partial p}{\partial\theta}\right)+v\frac{\partial}{\partial y}\left(\frac{\partial p}{\partial\theta}\right)+\frac{\partial p}{\partial\theta}\left(\frac{\partial u}{\partial x}+\frac{\partial v}{\partial y}\right)=0, \tag{10}$$

where curvature and certain Coriolis terms have been neglected and all horizontal velocities and gradients are defined with respect to an isentropic surface. Using the conventional Boussinesq-type assumption that compressible effects ($\partial\rho/\partial t$) are small in the Cartesian mass continuity equation but retaining thermodynamic effects due to compressibility, Eq. (10) becomes

$$\frac{\partial}{\partial t}\left(\frac{\partial Z}{\partial\theta}\right)+u\frac{\partial}{\partial x}\left(\frac{\partial Z}{\partial\theta}\right)+v\frac{\partial}{\partial y}\left(\frac{\partial Z}{\partial\theta}\right)+\frac{\partial Z}{\partial\theta}\left(\frac{\partial u}{\partial x}+\frac{\partial v}{\partial y}\right)=0. \tag{11}$$

Use of the above Boussinesq assumption avoids need of a double series expansion solution and does not alter the interpretation of the results to be made below.

Using the definition of the Montgomery streamfunction [Eq. (8)], the hydrostatic relationship (7) becomes

$$\partial M/\partial\theta=(1/\theta)(M-gZ). \tag{12}$$

The horizontal equations of motion [(5) and (6)], the hydrostatic relationship (12), and the mass continuity-thermodynamic equation (11) then form a complete set of equations with dependent variables u, v, M, Z. Interpretation of $\partial M/\partial\theta$ is facilitated by using the hydrostatic relationship in Cartesian coordinates and the definition of potential temperature in which case we obtain

$$\frac{\partial Z}{\partial\theta}=\frac{T}{\theta}\Big/(\Gamma_d-\gamma), \tag{13}$$

where Γ_d is the dry adiabatic lapse rate and $\gamma\equiv-\partial T/\partial Z$. Thus $\partial Z/\partial\theta$ can be interpreted as a temperature normalized with respect to the stratification.

To simplify the basic equations, we assume that the flow consists of small perturbations about a basic state of constant flow (zero vorticity):

$$\left.\begin{aligned} u&=\bar{U}+u'(x,y,\theta,t)\\ v&=v'(x,y,\theta,t)\\ M&=\bar{M}(\theta,y)+M'(x,y,\theta,t)\\ Z&=\bar{Z}(\theta,y)+Z'(x,y,\theta,t)\end{aligned}\right\}.$$

Substituting these definitions into (5), (6), (11) and (12) and neglecting products of perturbations, we obtain

$$\frac{\partial\bar{M}}{\partial x}=0, \tag{14a}$$

$$f\bar{U}=-\frac{\partial\bar{M}}{\partial y}=\text{constant}, \tag{14b}$$

$$\bar{M}-\theta\frac{\partial\bar{M}}{\partial\theta}=g\bar{Z}, \tag{14c}$$

$$\frac{\partial}{\partial t}\left(\frac{\partial\bar{Z}}{\partial\theta}\right)+\bar{U}\frac{\partial}{\partial x}\left(\frac{\partial\bar{Z}}{\partial\theta}\right)=0,$$

and

$$\frac{\partial u'}{\partial t}+\bar{U}\frac{\partial u'}{\partial x}-fv'=-\frac{\partial M'}{\partial x}, \tag{15a}$$

$$\frac{\partial v'}{\partial t}+\bar{U}\frac{\partial v'}{\partial x}+fu'=-\frac{\partial M'}{\partial y}, \tag{15b}$$

$$M'-\theta\frac{\partial M'}{\partial\theta}=gZ', \tag{15c}$$

$$\frac{\partial}{\partial t}\left(\frac{\partial Z'}{\partial\theta}\right)+\bar{U}\frac{\partial}{\partial x}\left(\frac{\partial Z'}{\partial\theta}\right)+u'\frac{\partial}{\partial x}\left(\frac{\partial\bar{Z}}{\partial\theta}\right)+v'\frac{\partial}{\partial y}\left(\frac{\partial\bar{Z}}{\partial\theta}\right)+\left(\frac{\partial\bar{Z}}{\partial\theta}\right)\left(\frac{\partial u'}{\partial x}+\frac{\partial v'}{\partial y}\right)=0. \tag{15d}$$

Operating on the basic state hydrostatic equation (14c) with $\partial^2/\partial\theta\partial x$ and using the basic state equations of motion (14b), we obtain

$$\left.\begin{aligned}\frac{\partial}{\partial x}\left(\frac{\partial\bar{Z}}{\partial\theta}\right)&=0\\ \left(\frac{\partial\bar{Z}}{\partial\theta}\right)&=\left(\frac{\partial\bar{Z}}{\partial\theta}\right)_{t=0}\end{aligned}\right\}, \tag{16}$$

in which case the perturbation mass continuity thermodynamics is simplified. To estimate the magnitude of various terms, we scale the variables as

$$\left.\begin{aligned}(x,y)&=L(\hat{x},\hat{y})\\ t&=\tau\hat{t}\\ \theta&=\Delta\theta\hat{\theta}+\theta_0\\ (u',v')&=\bar{U}(\hat{u},\hat{v})\\ M'&=fL\bar{U}\hat{M}\\ Z'&=\frac{\theta_0fL\bar{U}}{g\Delta\theta}\hat{Z}\end{aligned}\right\}, \tag{17}$$

where τ is the spin-down time scale to be estimated later, the scaling for M' is estimated by demanding the horizontal pressure gradient and Coriolis term be in rough balance, and the scaling for Z' is determined from hydrostatic balance. θ_0 represents the potential temperature at the bottom of the free layer while $\Delta\theta$ is the potential temperature thickness of the free layer influenced by boundary layer effects (to be estimated later). Employing scaling (17) and using (16), the perturbation equations become

$$\lambda\frac{\partial\hat{u}}{\partial\hat{t}}+\mathrm{Ro}\frac{\partial\hat{u}}{\partial\hat{x}}-\hat{v}=-\frac{\partial\hat{M}}{\partial\hat{x}}, \tag{18a}$$

$$\lambda\frac{\partial\hat{v}}{\partial\hat{t}}+\mathrm{Ro}\frac{\partial\hat{v}}{\partial\hat{x}}+\hat{u}=-\frac{\partial\hat{M}}{\partial\hat{y}}, \tag{18b}$$

$$\frac{\partial\hat{Z}}{\partial\hat{\theta}}=-\left(1+\frac{\Delta\theta}{\theta_0}\hat{\theta}\right)\frac{\partial^2\hat{M}}{\partial\hat{\theta}^2}, \tag{18c}$$

$$\lambda\frac{\partial}{\partial\hat{t}}\frac{\partial\hat{Z}}{\partial\hat{\theta}}+\mathrm{Ro}\frac{\partial}{\partial\hat{x}}\frac{\partial\hat{Z}}{\partial\hat{\theta}}+\frac{B^{-2}}{\left(1+\frac{\Delta\theta}{\theta_0}\hat{\theta}\right)}\left(\frac{\partial\hat{u}}{\partial\hat{x}}+\frac{\partial\hat{v}}{\partial\hat{y}}\right)=0, \tag{18d}$$

$$\lambda\equiv\frac{1}{f\tau},$$

$$\mathrm{Ro}\equiv\frac{\bar{U}}{fL},$$

$$B\equiv\frac{NfL}{g}\frac{\theta_0}{\Delta\theta},$$

$$N\equiv\left[\frac{g\frac{\overline{\partial\theta}}{\partial Z}}{\bar{\theta}(Z)}\right]^{\frac{1}{2}}.$$

The stability parameter B represents the relative importance of stratification and ultimately the importance of baroclinity. B appears in the denominator since $\partial\hat{Z}/\partial\hat{\theta}$ depends inversely on temperature. The stability parameter can also be viewed as the ratio of the horizontal length scale to the Rossby radius of deformation. In particular,

$$B=\frac{NfL}{g}\frac{\theta_0}{\Delta\theta}\sim\left[\frac{\frac{\Delta\theta}{g}H}{\theta_0}\right]^{\frac{1}{2}}\frac{fL}{g}\frac{\theta_0}{\Delta\theta}\sim L\left[\frac{f^2}{\frac{\Delta\theta}{g}H}{\theta_0}\right]^{\frac{1}{2}}\equiv\frac{L}{\lambda_R},$$

where H is the fluid depth and λ_R the Rossby radius of deformation. The length scales L and λ_R are generally not independent and in fact are considered to be typically O(1) for mid-latitude synoptic-scale systems. For example, if $g=10$ m s^{-2}, $\partial\bar{\theta}/\partial Z=4\times10^{-3}$ K m^{-1}, $L=10^6$ m, $f=10^{-4}$ s^{-1}, $\Delta\theta=50$ K and $\bar{T}=270$ K, then $N^{-1}\approx80$ s and $B\approx0.7$. We consider B to be O(1). To simplify the mathematics and emphasize the influence of boundary layer pumping, we presently assume that $\mathrm{Ro}\ll\lambda$. The assumption $\mathrm{Ro}/\lambda\ll1$ implies that $U\ll L/\tau$ which is equivalent to assuming that the basic flow is sufficiently weak or the length scale is sufficiently large. Then advections by the basic flow are small compared to local changes induced by boundary layer pumping. After focusing on the influence of boundary layer pumping in this section, we restore the influence of synoptic-scale accelerations in subsequent sections. We also implicitly assume that the spin-down time scale is small compared to the free flow diffusion time scale by virtue of the neglect of turbulent diffusion in the free-flow equations of motion. In summary

$$\mathrm{Ro}\ll\lambda\ll1$$

$$\frac{\Delta\theta}{\theta_0}\ll1$$

$$B\approx\mathrm{O}(1).$$

Examination of (18d) then indicates that, while $\partial\hat{u}/\partial\hat{x}$ and $\partial\hat{v}/\partial\hat{y}$ may each be O(1), their sum must be considerably smaller; in fact, the flow is nondivergent up to $\mathrm{O}(\lambda)$. It is then appropriate to expand flow variables in terms of a power series in λ as in Walin (1969). The zero- and first-order equations are

$$\hat{v}_0=\frac{\partial\hat{M}_0}{\partial\hat{x}}, \tag{19a}$$

$$\hat{u}_0=-\frac{\partial\hat{M}_0}{\partial\hat{y}}, \tag{19b}$$

$$\frac{\partial\hat{Z}_0}{\partial\hat{\theta}}=-\left(1+\frac{\Delta\theta}{\theta_0}\hat{\theta}\right)\frac{\partial^2\hat{M}_0}{\partial\hat{\theta}^2}, \tag{19c}$$

$$\frac{B^{-2}}{\left(1+\frac{\Delta\theta}{\theta_0}\hat{\theta}\right)}\left(\frac{\partial\hat{u}_0}{\partial\hat{x}}+\frac{\partial\hat{v}_0}{\partial\hat{y}}\right)=0, \tag{19d}$$

and

$$\frac{\partial\hat{u}_0}{\partial\hat{t}}-\hat{v}_1=-\frac{\partial\hat{M}_1}{\partial\hat{x}}, \tag{20a}$$

$$\frac{\partial\hat{v}_0}{\partial\hat{t}}+\hat{u}_1=-\frac{\partial\hat{M}_1}{\partial\hat{y}}, \tag{20b}$$

$$\frac{\partial\hat{Z}_1}{\partial\hat{\theta}}=-\left(1+\frac{\Delta\theta}{\theta_0}\hat{\theta}\right)\frac{\partial^2\hat{M}_1}{\partial\hat{\theta}^2}, \tag{20c}$$

$$\frac{\partial}{\partial\hat{t}}\left(\frac{\partial\hat{Z}_0}{\partial\hat{\theta}}\right)+\frac{B^{-2}}{\left(1+\frac{\Delta\theta}{\theta_0}\hat{\theta}\right)}\left(\frac{\partial\hat{u}_1}{\partial\hat{x}}+\frac{\partial\hat{v}_1}{\partial\hat{y}}\right)=0, \tag{20d}$$

where the subscript is the expansion index. Combining the first-order equations (20a)–(20d), assuming B to be independent of height, and using (19a)–(19c), we obtain for the zeroth order streamfunction

$$\frac{\partial}{\partial \hat{t}}\left[\frac{\partial^2 \hat{M}_0}{\partial \hat{x}^2}+\frac{\partial^2 \hat{M}_0}{\partial \hat{y}^2}+B^2\left(1+\frac{\Delta\theta}{\theta_0}\hat{\theta}\right)^2\frac{\partial^2 \hat{M}_0}{\partial \hat{\theta}^2}\right]=0. \quad (21)$$

Eq. (21) is a linearized version of the quasi-geostrophic potential vorticity equation in that advections are not included. As a result of the above-mentioned Boussinesq assumption and above linearization, this equation is simpler than the potential vorticity equation used by Bleck (1973) for numerical application to actual cyclogensis.

b. Boundary layer pumping

We presently specify the boundary conditions and initial conditions for the potential vorticity equation which is elliptic in $\partial \hat{M}_0/\partial \hat{t}$. The boundary layer pumping expression (2) is employed as a lower boundary condition by taking the Lagrangian derivative of the perturbation hydrostatic relationship in which case

$$\frac{d}{dt}\left(M'-\theta\frac{\partial M'}{\partial \theta}\right)=g\frac{dZ'}{dt}. \quad (22)$$

Assuming for the moment that the vertical motion at the top of the boundary layer is due exclusively to boundary layer pumping (level terrain), combining (2) and (22), scaling according to (17), allowing $\mathrm{Ro}\to 0$, multiplying through by $\Delta\theta/\theta_0$ and rearranging, we obtain

$$\lambda\frac{\partial}{\partial \hat{t}}\left[\frac{\Delta\theta}{\theta_0}\hat{M}-\left(1+\frac{\Delta\theta}{\theta_0}\hat{\theta}\right)\frac{\partial \hat{M}}{\partial \hat{\theta}}\right]=\frac{gF}{f^2L^2}\frac{\Delta\theta}{\theta_0}\left(\frac{\partial^2 \hat{M}}{\partial \hat{x}^2}+\frac{\partial^2 \hat{M}}{\partial \hat{y}^2}\right), \quad \hat{\theta}=0. \quad (23)$$

O(Ro) corrections to boundary layer pumping are neglected since this vertical motion is itself a first-order contribution to the free flow dynamics. Scaled variables are O(1) and $\Delta\theta/\theta_0 \ll 1$, so that for atmospheric flow problems the primary balance is

$$-\lambda\frac{\partial}{\partial \hat{t}}\frac{\partial \hat{M}}{\partial \hat{\theta}}\approx\frac{gF}{f^2L^2}\frac{\Delta\theta}{\theta_0}\left(\frac{\partial^2 \hat{M}}{\partial \hat{x}^2}+\frac{\partial^2 \hat{M}}{\partial \hat{y}^2}\right).$$

This balance implies that for a hypothetical "stratified-barotropic" atmosphere, where vorticity is independent of θ, the spin-down time scale is

$$\tau=\frac{fL^2}{gF}\frac{\theta_0}{\Delta\theta}.$$

Choosing this time scale to be the scaling time scale and expanding the flow in terms of λ, as above, we obtain the following zero-order lower boundary condition:

$$\frac{\partial}{\partial \hat{t}}\left[\frac{\Delta\theta}{\theta_0}\hat{M}_0-\left(1+\frac{\Delta\theta}{\theta_0}\hat{\theta}\right)\frac{\partial \hat{M}_0}{\partial \hat{\theta}}\right]=\frac{\partial^2 \hat{M}_0}{\partial \hat{x}^2}+\frac{\partial^2 \hat{M}_0}{\partial \hat{y}^2}, \quad \hat{\theta}=0. \quad (24)$$

c. Solution

By employing the coordinate transformation

$$\eta=\ln\left(1+\frac{\Delta\theta}{\theta_0}\hat{\theta}\right),$$

Eqs. (21), (24), (25) transform to

$$\frac{\partial}{\partial \hat{t}}\left[\frac{\partial^2 \hat{M}_0}{\partial \hat{x}^2}+\frac{\partial^2 \hat{M}_0}{\partial \hat{y}^2}+\left(\frac{gN^{-1}}{fL}\right)^{-2}\left(\frac{\partial^2 \hat{M}_0}{\partial \eta^2}-\frac{\partial \hat{M}_0}{\partial \eta}\right)\right]=0,$$

$$\frac{\partial}{\partial \hat{t}}\left(\hat{M}_0-\frac{\partial \hat{M}_0}{\partial \eta}\right)=\frac{\theta_0}{\Delta\theta}\left(\frac{\partial^2 \hat{M}_0}{\partial \hat{x}^2}+\frac{\partial^2 \hat{M}_0}{\partial \hat{y}^2}\right) \quad \text{at } \eta=0,$$

$$\hat{M}_0\to 0;\ \eta=\ln\left(\frac{\theta_0+\Delta\theta}{\theta_0}\right).$$

We can examine the decay of vorticity with time and the decrease of the spin-down influence with height by imposing harmonic side boundary conditions and assuming that the influence of boundary layer pumping vanishes at dimensional potential height $\theta=\theta_0+\Delta\theta$ so that

$$\hat{M}_0(\hat{\theta}=1)=0. \quad (25)$$

We can then separate horizontal and vertical dependencies by Fourier transforming the streamfunction with respect to horizontal distance, i.e.,

$$\hat{M}_0(\hat{x},\hat{y},\hat{\theta},\hat{t})=\hat{m}(\hat{\theta},\hat{t})\ \mathrm{Re}\{\exp[i(\hat{k}\hat{x}+\hat{l}\hat{y}]\}.$$

The initial condition is then

$$\hat{M}_0(\hat{x},\hat{y},\hat{\theta},0)=\hat{m}(\hat{\theta},0)\ \mathrm{Re}\{\exp[i(\hat{k}\hat{x}+\hat{l}\hat{y})]\}.$$

The system would become mathematically equivalent to Walin's equations if we replace θ with a constant value $\tilde{\theta}$ whenever it appears as a coefficient and if we assume that $\Delta\theta/\theta \ll 1$. While we find it not necessary to invoke these assumptions, it will turn out that the additional generality makes little qualitative difference. The above system is then converted to an ordinary differential equation by Laplace transforming the time dependence. After solving the resulting ordinary differential equation, applying the inverse transform, using the residual theorem, converting back to dimensional variables and allowing $\Delta\theta$ to approach a sufficiently large value so that influences of the upper boundary vanish, we obtain

$$M_0(x,y,\theta,t;k,l)=\mathrm{Re}\{\exp[i(kx+ly]\}$$
$$\times\{m(\theta,0)-m(0,0)[1-\exp(-t/t_e)](\theta/\theta_0)^{(1-\alpha)/2}\}, \quad (26)$$

where

$$\hat{r}^2 \equiv l^2 + k^2,$$

$$t_e \equiv \frac{\frac{1}{2} f(1+\alpha)}{F g \hat{r}^2},$$

$$\alpha \equiv \left[1 + \left(\frac{2\hat{r}g}{Nf}\right)^2\right]^{\frac{1}{2}},$$

where k and l are horizontal wavenumbers and t_e is the stratified spin-down time scale. As $t/t_e \to$ large, the perturbation flow has been spun down to negligibly small values by boundary layer pumping. In the absence of boundary layer pumping, the amplitude of the flow does not change with time. With increasing stratification (increasing Brunt-Väisälä frequency N), the spin-down time scale decreases. This is a reflection of the fact that with increased stratification, the circulation induced by boundary layer pumping is increasingly bottom trapped, thus increasing the divergence and rate of pressure adjustments immediately above the boundary layer. In other words, with greater stratification, the fluxes out of the boundary layer are absorbed by a thinner free layer so that the secondary circulation and vorticity adjustments immediately above the boundary layer are faster. The spin-down time scale also decreases with decreasing length scale. The greater the horizontal length scale, the greater the time scale for a parcel following the frictionally driven secondary circulation to complete one cycle. Thus, as the length scale increases or as the stratification decreases, the relative importance of frictionally induced pressure adjustments and, therefore, the spin-down rate decreases.

The spin-down time scale expression can be simplified by noting that $(2\hat{r}g/fN) \gg 1$ for most mid-latitude synoptic flows. For example, for $f = 10^{-4}$ s^{-1}, $N^{-1} = 80$ s (Section 3a), and for a horizontal wavelength (e.g., distance between two low pressure centers) of $L = 2\pi/\hat{r} = 2 \times 10^6$ m,

$$\frac{2\hat{r}g}{fN} \approx 50.$$

Then, except in the case of very strong stratification, we have approximately

$$t_e = \frac{N^{-1}}{F\hat{r}}. \tag{27}$$

The spin-down rate $(1/t_e)$ is proportional to the stratification and the boundary layer pumping efficiency and inversely proportional to the length scale of the flow. The spin-down time scale can be expected to range from $\sim\frac{1}{2}$ day for $N^{-1} = 60$ s, $F = 250$ m, $L = 10^6$ m to almost 20 days for $N^{-1} = 100$ s, $F = 40$ m, $L = 4 \times 10^6$ m. If the initial perturbation streamfunction is independent of elevation $m(\theta,0) = m(0,0)$, the percentage decrease of lower tropospheric vorticity due to boundary layer pumping is $\exp(-T/t_e)$ after one synoptic time scale T. For the above two numerical examples, the reduction of vorticity at the bottom of the free flow after 3 days ranges from substantial destruction to almost no effect. In other words, large variations in the importance of boundary layer pumping can be expected due in part to the fact that the surface stress can vary by an order of magnitude depending on surface roughness, boundary layer stratification and wind speed. For conditions thought to be typical of an average extratropical cyclone (Figs. 2 and 3), the vorticity in the lower part of the free flow is significantly reduced on a synoptic time scale. The above simplified theory then indicates that boundary layer pumping can significantly alter the vorticity in the lower troposphere on a synoptic time scale particularly under conditions of large surface stress and large free flow stratification.

As is evident from (26), the effects of boundary layer pumping decrease rapidly with elevation. We define the penetration depth scale to be the depth at which the vorticity destruction rate is reduced to $1/e$ of its value immediately above the boundary layer. The potential temperature thickness of this depth is

$$(\theta - \theta_0) = \theta_0\{\exp[-2/(1-\alpha)] - 1\} \tag{28}$$

Using the above assumption that $2\hat{r}g/fN \gg 1$ and the definition of α and N, this depth scale (28) is approx-i mately

$$(\theta - \theta_0) = \theta_0\left(\frac{f}{\hat{r}g}\right)\left[\frac{g}{\bar{\theta}(Z)}\frac{\partial\bar{\theta}}{\partial Z}\right]^{\frac{1}{2}}. \tag{29}$$

The actual penetration depth is approximately

$$H \approx \frac{f}{\hat{r}}\left(\frac{\bar{\theta}(Z)}{g}\right)^{\frac{1}{2}}\left(\frac{\partial\bar{\theta}}{\partial Z}\right)^{-\frac{1}{2}} = \frac{f}{\hat{r}N}. \tag{30}$$

Thus, the penetration depth scale for the above atmospheric flow situation is inversely proportional to the square root of the stratification and proportional to the length scale of the flow. The same tendencies are predicted by Walin's analyses. This depth scale is an intrinsic property of the stratified free flow and does not depend on the nature of the boundary layer pumping. For example, this depth scale is the same for any type of forcing at the bottom of a stratified layer or sublayer as can be shown by redoing the analyses leading to (26) with constant forcing. A similar decrease with height of the influence of forcing in a stratified flow is evident in Kuo's (1956) analyses of the distribution of the "influence function" of point forcing. The constraining influence of stratification on topographical forcing is examined by Hogg (1973).

The depth scale describing the portion of the fluid significantly influenced by boundary layer pumping increases with time and is proportional to the above

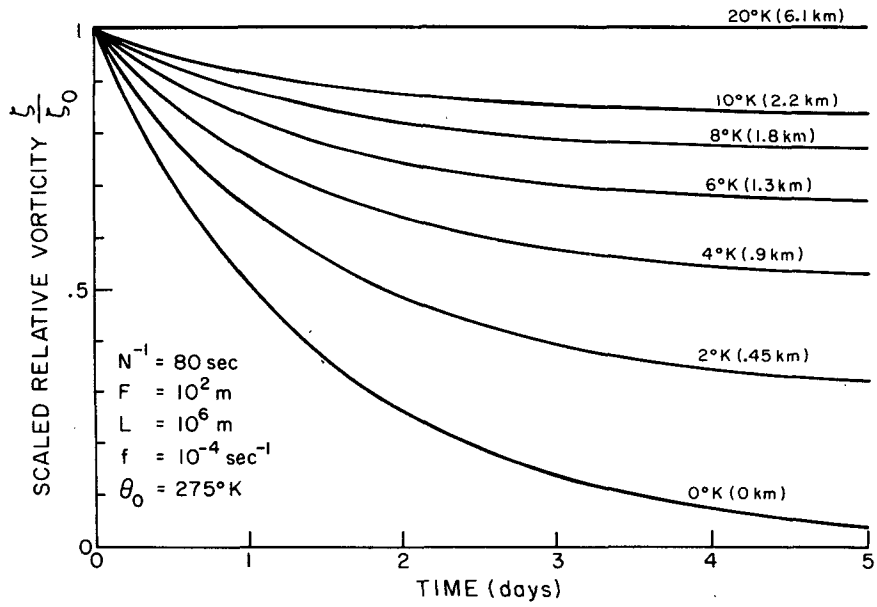

FIG. 2. Spin-down of relative vorticity (scaled with respect to the height-independent initial value) at different levels in the free flow. Plots are labelled according to their potential temperature excess and elevation above the boundary layer top. The latter is computed using the relationship leading to (30).

penetration depth scale modulated by an exponential time dependency evident from (26) or Figs. 2–3. For $f=10^{-4}$ s^{-1}, H varies from 1 km for $L=10^6$ m and $N^{-1}=60$ s to $\sim 6\frac{1}{2}$ km for $L=4\times10^6$ m and $N^{-1}=100$ s. These calculations indicate that boundary layer pumping is likely to influence only a fraction of the troposphere for small length scale circulations with significant stratification and perhaps all of the troposphere with larger length scale circulations with weak stratification. In the event the free-flow depth scale is small enough to be comparable to the boundary layer depth, then the "boundary layer approximation" leading to (1) may break down depending on boundary layer stratification. Furthermore, the quasi-geostrophic assumption may be invalid in such a thin free flow since the free flow divergence becomes comparable to the frictionally driven convergence.

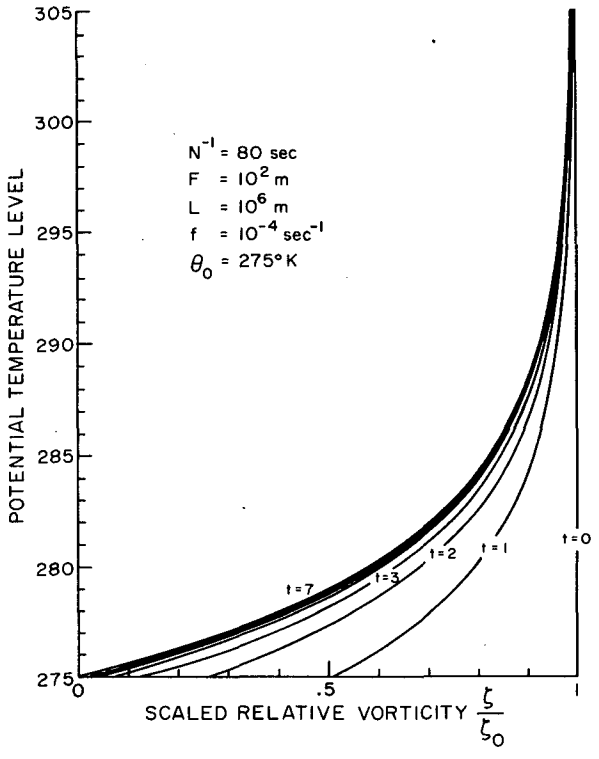

FIG. 3. Spin-down of scaled relative vorticity. Plots are labelled according to number of days after initiation of spin-down.

It is difficult to compare the above estimates with actual atmospheric observations since a number of mechanisms in addition to boundary layer pumping are operating simultaneously. Although somewhat inconclusive, the case study of Graystone (1962) indicates that boundary layer pumping could be synoptically important. The troposphere can be viewed as a statistical upper boundary to the direct influence of forcing at the earth's surface. However, in a given situation, the primary influence of nonconvective vertical motions near the earth's surface may be confined to a substantially thinner layer. In summary, we suggest that boundary layer pumping is likely to be important in synoptic circulations of strong stratification and small horizontal length scale. In this case, mass fluxes out of the boundary layer are concentrated in the lower troposphere. In terms of the length scale over which the flow varies by one amplitude, which is one-fourth of the wavelength for periodic flow, the importance of boundary layer pumping is described by the depth scale fL/N and time scale L/FN.

4. Scale analysis for accelerated, forced flow

The influence of accelerations on the role of boundary layer pumping can be examined with the model in the previous section by considering fixed relationships between λ and Ro and employing a double series expansion or finite differencing approach. However, a more straightforward and perhaps more illuminating estimate of the influence of accelerations can be achieved by considering a simple homogeneous fluid of depth comparable to the stratified flow penetration depth derived in the previous section [see Eq. (30)]. By choosing this depth, the possible importance of various acceleration effects in the atmosphere can be estimated.

A homogeneous, hydrostatic, frictionless free layer conserves potential vorticity as can be shown by combining the vorticity and mass continuity equations (e.g., Batchelor, 1970), in this case we have

$$\frac{d}{dt}(\zeta+f)=\frac{(\zeta+f)}{H}\left(\frac{dH_T}{dt}-\frac{dH_B}{dt}\right), \tag{31a}$$

or alternatively

$$\frac{d}{dt}\left(\frac{\zeta+f}{H}\right)=0, \tag{31b}$$

where ζ is the relative vorticity, H the variable depth of the fluid, $(\zeta+f)/H$ is referred to as the potential vorticity, and H_T and H_B are, respectively, the elevations of the upper and lower boundaries of the free layer which are both substantial surfaces. In the present study, we consider the flow situation where H_T is constant and H_B varies due to 1) specified externally forced vertical motion A as would be generated, for example, by flow over varying terrain height, and 2) frictionally driven convergence or divergence. Employing the boundary layer vertical motion expression [Eq. (2)] and again assuming constant Coriolis parameter, the above vorticity equation becomes

$$\frac{d\zeta}{dt}=-\left(\frac{\zeta+f}{H}\right)(F\zeta+\mathrm{Ro}w_1+A). \tag{32}$$

We define the following scales describing externally forced synoptic-scale flow: L is the horizontal length scale of the flow of typical magnitude of 2000 km; then the terrain slope of interest is h^*/L, where h^* is the bulk surface elevation change over the synoptic length scale. Here we do not consider interactions with sub-synoptic, terrain-induced circulations (Sawyer, 1959) such as internal gravity waves (e.g., Klemp and Lilly, 1975) and small-scale low-level "deflection" or "blocking" (e.g., Newton 1956). In addition to the upstream inflow velocity U, the flow is characterized by the perturbation velocity scale V. Divergence and vorticity then scale like V/L.

Based on calculations in the previous section, we assume that the spin-down time scale is comparable to or longer than the synoptic time scale T. Then temporal and advective accelerations scale like

$$\frac{\partial \mathbf{V}}{\partial t}\sim\frac{V}{T},$$

$$\mathbf{V}\cdot\nabla\mathbf{V}\sim\frac{UV}{L}.$$

Since the synoptic time scale is typically larger than the parcel time scale L/U (e.g., $L\sim 2\times10^6$ m, $U\sim 20$ m s^{-1}, then $L/U\sim 1$ day), temporal accelerations will be generally smaller than advective accelerations. In the "slow flow" case, where the inflow velocity is small compared to the disturbed velocity, then U in the present analysis can be assigned to be V. The ratio of the total acceleration term to the Coriolis term is

$$\mathrm{Ro}\equiv\frac{V}{fL}\sim\zeta/f\ll 1. \tag{33}$$

The quasi-geostrophic assumption (Ro$\ll$1) also imposes restrictions on the terrain forced vertical motions as can be shown from the approximate frictionless quasi-geostrophic version of the vorticity equation (32):

$$\frac{d\zeta}{dt}\sim f\frac{\bar{A}}{\bar{H}}, \tag{34}$$

where $\bar{A}$ and $\bar{H}$ are, respectively, the average forcing vertical motion and average free-flow depth. The vorticity externally generated during the Lagrangian time scale L/U then scales like

$$\bar{\zeta}=\frac{f\bar{A}L}{\bar{H}U}, \tag{35}$$

in which case the Rossby number becomes

$$\mathrm{Ro}=\frac{\bar{A}L}{\bar{H}U}. \tag{36}$$

For topographically forced flow where $\bar{A}\sim Uh^*/L$,

$$\bar{\zeta}=\frac{fh^*}{\bar{H}}, \tag{37}$$

$$\mathrm{Ro}=\frac{h^*}{\bar{H}}. \tag{38}$$

Thus, quasi-geostrophic theory can be applied to flow cases where the terrain height is small compared to the free flow depth scale (Phillips, 1963). Conversely, the relative importance of orographic effects is indicated by the ratio of the terrain depth scale to the appropriate free-flow depth scale.

Scaling the vorticity with $(\bar{A}/\bar{H})(fL/U)$, time with L/U, vertical motions A and w with $\bar{A}$, and free-flow depth with $\bar{H}$, the vorticity equation with error $O(Ro^2)$ becomes

$$\frac{d\hat{\zeta}}{d\hat{t}}=-\frac{(Ro\hat{\zeta}+1)}{\hat{H}}(F^*\hat{\zeta}+Ro\hat{w}_1+\hat{A}), \tag{39}$$

where

$$F^*\equiv\frac{C_DL}{\bar{H}}\Big/(1+\hat{C}_D^2).$$

All dependent variables in (39) are expected to be O(1). The vorticity dynamics then depend on the Rossby number and the boundary layer parameter F^*. The latter represents the relative importance of boundary layer mass convergence. Noting that generally $\hat{C}_D\ll 1$ (Section 2), then $F^*\approx C_DL/\bar{H}$ and can be expected to be typically $O(10^{-1})$–O(1) depending on the surface drag coefficient and free-flow depth scale In this respect, the above scale analysis differs from that of the quasi-geostrophic theory of tropospheric planetary waves of Phillips (1963), where F^* was considered to be O(Ro). In that case the contribution due to boundary layer pumping would be a factor of Rossby number smaller. F^* is largest and boundary layer pumping is most important for 1) large pumping efficiency F, that is, large surface stress such as might occur with strong winds and/or large surface drag coefficient, 2) small free-flow depth in which case the free flow is more sensitive to mass fluxes from the boundary layer, and 3) large horizontal length scale where a given boundary layer pumping rate has more time to influence a fluid element.

The conventional quasi-geostrophic solution can be computed from (39) by letting $Ro\to 0$. That is, we have already divided through once by the Rossby number in the algebra leading to (39) so that (39) contains first-order corrections to the quasi-geostrophic theory of Ingersoll (1969) and Huppert and Stern (1974). In the next section we examine the influence of such accelerations from a Lagrangian point of view.

5. Lagrangian solution

We now examine the influence of boundary layer pumping and accelerations on the Lagrangian evolution of the relative vorticity. Since the Lagrangian derivative contains nonlinear components, order-of-Rossby-number corrections to frictionally driven mass convergence can be most conveniently calculated for well-mixed flows. Relaxation of the well-mixed assumption requires additional assumptions (Mahrt, 1975) and will presently not be considered. Following a procedure outlined in Mahrt (1975), we 1) layer-integrate the boundary layer equations of motion, 2) assume a linearized surface drag relationship, 3) scale the equations in accordance with Section 4 and expand the horizontal velocity in terms of the Rossby number, and 4) layer-integrate the mass continuity equation. The O(Ro) correction to the vertical motion at the boundary layer top, scaled with respect to the externally forced vertical motion $\bar{A}$, is then

$$\left.\begin{aligned}\hat{w}_1&=h\frac{(1-\hat{C}_D^2)}{(1+\hat{C}_D^2)^2}\frac{d\hat{\zeta}_g}{d\hat{t}}\\ \hat{h}&\equiv\frac{h}{\bar{H}}\frac{1}{Ro}\sim\frac{h}{h^*}\end{aligned}\right\}, \tag{40}$$

where h is again the depth of the boundary layer. Both h and C_D are assumed to be constant in the above vertical motion calculation. The relationship between h and h^* makes use of (37). We normally expect the boundary layer depth to be small compared to the free-flow depth scale, fortuitously O(Ro) for quasi-geostrophic atmospheric flow. Then $\hat{h}$ is O(1) and $Ro\hat{w}_1$ is truly an O(Ro) correction to the boundary layer pumping. If $h/\bar{H}$ approaches O(1), the average first-order divergence in the free layer is comparable to the frictionally driven convergence in the boundary layer and the flow may no longer remain in quasi-geostrophic balance.

Since the scaled drag coefficient $\hat{C}_D$ is generally small compared to 1 (Section 2), the correction term for boundary layer accelerations is due primarily to "frictionless effects"; that is, the acceleration-modification of the boundary layer divergence is only weakly modified by frictional effects and is thus comparable to the free-flow divergence. In particular for $\hat{C}_D<1$, the acceleration-modification of the boundary layer pumping rate generates an influence mathematically analagous to increasing the depth of the free flow by an amount something less than the boundary layer depth. In the less common atmospheric case $\hat{C}_D>1$, this effect is actually analogous to decreasing the depth of the free flow since the net acceleration correction to the boundary layer divergence is of opposite sign to that of the free-flow divergence. We formalize this similarity by defining an effective free-flow depth

$$H^*\equiv\hat{H}+Ro\hat{h}\frac{(1-\hat{C}_D^2)}{(1+\hat{C}_D^2)^2}.$$

Then combining (39) and (40) we obtain

$$H^*\frac{d\hat{\zeta}}{d\hat{t}}\approx-(Ro\hat{\zeta}+1)[F^*\hat{\zeta}+\hat{A}(\hat{t})]. \tag{41}$$

For a given forcing $\hat{A}(\hat{t})$, increases in the effective depth H^* due to accelerations in the boundary layer decreases the vorticity production rate. Accelerations above the boundary layer influence the vorticity adjustment rate through the influence of relative vorticity on the absolute vorticity $Ro\hat{\zeta}+1$.

Neglecting variations of the scaled drag coefficient

C_D and noting from (31b) that the modified potential vorticity $(\hat{\zeta}\mathrm{Ro}+1)/H^*$ is then conserved, the solution to (41) is easily found to be

$$\left.\begin{aligned}\hat{\zeta}&=\hat{\zeta}(0)\exp[-\tilde{F}\hat{t}]\\&\quad-\exp[-\tilde{F}\hat{t}]\int_0^{\hat{t}}\exp[\tilde{F}\hat{t}]\hat{A}(\hat{t})(\tilde{F}/F^*)d\hat{t}\\ \tilde{F}&=\left[\frac{\mathrm{Ro}\hat{\zeta}(0)+1}{H^*(0)}\right]F^*.\end{aligned}\right\}\quad(42)$$

Positive initial relative vorticity speeds up the vortex stretching rate and thus decreases the adjustment time scale. In the case of constant external forcing, zero initial relative vorticity and momentarily choosing $\hat{H}$ such that $H^*(0)=1$, the scaled vorticity solution (42) simplifies to

$$\hat{\zeta}=-(\hat{A}/F^*)[1-\exp(-\tilde{F}\hat{t})],\quad \hat{A}=\pm 1.$$

In this simplified case, the adjustment rate is proportional to the frictional parameter F^* while the steady-state vorticity is inversely proportional to the frictional parameter. Of course, the vorticity at a given point in time decreases with increasing frictional parameter.

6. Steady flow

We now consider steady flow from an Eulerian point of view in order to examine the spatial distribution of the relative vorticity with respect to the forcing field or orography. Assuming steady state and invariance in one horizontal direction, we have

$$\frac{d}{dt}=u\frac{\partial}{\partial x}.\quad(43)$$

Since we wish to examine the influence of boundary layer pumping and accelerations on synoptic-scale flow, we scale length by the synoptic length scale L. The horizontal distance required for boundary layer pumping to spin-down the vorticity of a moving fluid element or system is quite variable and may be much larger than the synoptic length scale. This variability can be argued from the substantial variation of spin-down time scales estimated in Section 3. We scale the advecting velocity by the inflow velocity U which in the subsequent development is considered to be at least as large as the disturbed velocity. The vorticity equation (39) with (43) then becomes

$$\hat{H}\hat{u}\frac{\partial}{\partial\hat{x}}\hat{\zeta}=-(\mathrm{Ro}\hat{\zeta}+1)[F^*\hat{\zeta}+\mathrm{Ro}\hat{w}_1+\hat{A}(\hat{x})],\quad(44)$$

where $\hat{w}_1$ is now the contributions of advective accelerations to boundary layer vertical motions. Noting that two-dimensional mass continuity demands that

$$\hat{H}\hat{u}=\hat{H}(0)\hat{u}(0),$$

the vorticity equation (44) reduces to

$$\hat{H}(0)\hat{u}(0)\frac{\partial}{\partial\hat{x}}\hat{\zeta}=-(\mathrm{Ro}\hat{\zeta}+1)[F^*\hat{\zeta}+\mathrm{Ro}\hat{w}_1+\hat{A}(\hat{x})].\quad(45)$$

The O(Ro) influence of advective accelerations on boundary layer vertical motions can be computed by the same procedure leading to (40). After neglecting terms of $O(\mathrm{Ro}^2)$, we obtain

$$\hat{w}_h\approx F^*\hat{\zeta}_g-\mathrm{Ro}F^*\frac{(1-\hat{C}_D{}^2)}{(1+\hat{C}_D{}^2)}\hat{\zeta}_g{}^2+\mathrm{Ro}\hat{h}\frac{(\hat{u}_g-\hat{C}_D\hat{v}_g)}{(1+\hat{C}_D{}^2)^2}\frac{\partial}{\partial\hat{x}}\hat{\zeta}_g.\quad(46)$$

As discussed in Mahrt (1975), the advective modification term with quadratic dependence on vorticity acts to reduce the boundary layer vertical motion with positive vorticity and vice versa. The vorticity advection-like term acts to shift the maximum boundary layer vertical motion upstream from the vorticity maximum advection. It is useful to combine the boundary layer vorticity advection term with that of the free flow by again defining an effective flow depth

$$H^*\equiv\hat{H}(0)+\mathrm{Ro}\hat{h}\frac{(\hat{u}_g-\hat{C}_D\hat{v}_g)}{\hat{u}(0)(1+\hat{C}_D{}^2)^2}=\hat{H}(0)+\frac{h}{\bar{H}}\frac{(\hat{u}_g-\hat{C}_D\hat{v}_g)}{\hat{u}(0)(1+C_D{}^2)^2},\quad(47)$$

where $\hat{h}$ is generally O(1) as discussed earlier. In general, the effect of boundary layer accelerations again increase the effective flow depth by something less than the boundary layer depth. The scaled geostrophic wind component $\hat{u}_g$ is constant since we have assumed constant Coriolis parameter and invariance in the y direction. In the subsequent development we linearize the vorticity equation by neglecting the generally small variations of H^* due to variations of $\hat{C}_D\hat{v}_g$. This assumption is satisfied if either the flow changes due to forcing are small compared to the inflow or if $\hat{C}_D\ll 1$. Using the above definition of the effective depth H^* [Eq. (47)] and the boundary layer vertical motion expression (46), the vorticity equation (45) then becomes

$$\frac{\partial\hat{\zeta}}{\partial\hat{x}}=-\hat{A}(\hat{x})-[F^*+\mathrm{Ro}\hat{A}(\hat{x})]\hat{\zeta}-\mathrm{Ro}F^*\bar{C}_D{}^2\hat{\zeta}^2,\quad(48)$$

where terms of $O(\mathrm{Ro}^2)$ have been neglected and for notation brevity we have redefined the nondimensional drag coefficient to be

$$\bar{C}_D{}^2\equiv\frac{2\hat{C}_D{}^2}{1+\hat{C}_D{}^2},$$

and have specified the advecting velocity scale to be

$$U \equiv H^* u(0).$$

The selection of U is reasonable since for quasi-geostrophic flow, the non-dimensional constant H^* is close to unity. As before, the vorticity equation reduces to the classical quasi-geostrophic vorticity equation if terms of order Ro are neglected. Since we expect the frictional parameter F^* to be typically $O(10^{-1})$ [although occasionally as large as $O(1)$] and expect $\hat{C}_D$ and therefore $\tilde{C}_D$ to be typically $O(10^{-1})$, we interpret (48) by momentarily considering F^* and $\tilde{C}_D$ to be less than, say $\frac{1}{2}$.

The largest modification due to accelerations is then the influence of absolute vorticity changes on the externally forced vortex stretching which is the term $\mathrm{Ro}\hat{A}(\hat{x})\hat{\zeta}$. For example, with positive relative vorticity, such as is produced in downslope flow, vorticity production is increased. Conversely, the vorticity production is decreased in upslope flow. McClain (1960) suggests that this effect may be in part responsible for the frequent cyclogenesis downstream from the Western Cordillera (Rockies, Sierra-Cascade ranges, etc.,) and apparent absence of a maximum frequency of anticyclonic circulations in the rising motion upstream from the Western Cordillera.

This "frictionless" acceleration effect, however, is modulated by a generally smaller acceleration-modification of that portion of the vortex stretching induced by boundary layper pumping. This modification is due to three contributions:

1) Modification of the absolute vorticity due to free-flow accelerations changes the influence of a given boundary layer pumping rate on the vorticity dynamics. This contribution is $\mathrm{Ro}F^*\hat{\zeta}^2$ [(45) and (46)].

2) Accelerations in the boundary layer modify the boundary layer pumping rate. This modification is $[-F^*\mathrm{Ro}(1-\hat{C}_D^2)\hat{\zeta}^2]/(1+\hat{C}_D^2)$. This second effect often nearly cancels the first effect leaving a generally small residual $\mathrm{Ro}F^*\tilde{C}_D^2\hat{\zeta}^2$.

3) A third acceleration effect in the boundary layer, associated with vorticity advection in the boundary layer, is often only weakly affected by "frictional influences" and is viewed here as an increase in the "effective" depth of the free flow [Eq. (47)]. This contribution acts to decrease the dimensional vorticity changes.

In summary the net effect of interactions between accelerations and boundary layer pumping (effects 1 and 2) appear to be important only under conditions of strong surface stress or thin boundary layer and free-flow depths or small Coriolis parameter as can be seen by examining (4), (39) and (48). In particular, such interactions are important only when $F^*\tilde{C}_D^2 \sim O(1)$. An example of such conditions would be $C_D = 4\times10^{-3}$, $U = 10$ m s^{-1}, $f = 10^{-4}$ s^{-1}, $h = 500$ m, $L = 10^3$ km and $H = 3$ km. In general the most important influences on the vorticity field are due to unmodified boundary layer pumping and to variations of absolute vorticity associated with free-flow accelerations. In cases of positive relative vorticity, such as might occur with forced subsidence as in downslope flow, accelerations increase the absolute vorticity and vorticity production. Such an increased vorticity production rate is opposed by vorticity destruction due to boundary layer pumping. With negative relative vorticity such as might be produced with forced rising motion, both free flow accelerations and boundary layer pumping act to reduce the vorticity production. Thus for a given forcing magnitude, the net vorticity production is largest in the case of forced subsidence.

For negligible upstream relative vorticity, the frictionally driven vertical motion will oppose the externally forced vertical motion. Therefore, for a given slope magnitude, vertical motions are greater in upslope flow where geostrophic vorticities and Ekman pumping are weakest.

To illustrate these tendencies we present a numerical example. Consider a slope of 10^{-3}, $f = 10^{-4}$ s^{-1}, $L = 10^6$ m, $H = 5$ km, $C_D = 1.5\times10^{-3}$, $\hat{C}_D = 0.1$ (see Section 2). Then from Eqs. (37), (39) and (48), we have

$$\mathrm{Ro} = 0.2, \quad F^* = 0.3, \quad \tilde{C}_D = 0.2.$$

In this case the scaled free-flow acceleration contribution is $\sim 0.2\hat{\zeta}$, the boundary layer pumping term is $\sim 0.3\hat{\zeta}$ while the interaction term between accelerations and boundary layer pumping is $O(10^{-3})\hat{\zeta}^2$. Thus in downslope flow with the above approximate conditions, acceleration and boundary layer pumping terms partially cancel in which case the vorticity production can be estimated reasonably well from quasi-geostrophic frictionless theory. On the other hand, in upslope flow, accelerations and boundary layer pumping combine to significantly reduce the net vorticity production. Of course, in individual flow situations the upstream relative vorticity may be of major importance.

a. Constant forcing

In the case of constant forcing, the vorticity equation (48) can be solved by using the transformation

$$\hat{\zeta} = (\mathrm{Ro}F^*\tilde{C}_D^2\eta)^{-1}(\partial\eta/\partial\hat{x}).$$

After solving the transformed equation and applying the inverse transform, we obtain for $\hat{A}(\hat{x}) = \pm 1$:

$$\left.\begin{aligned} \hat{\zeta} &= -(2\,\mathrm{Ro}F^*\tilde{C}_D^2)^{-1}[C(\mathrm{Ro}\hat{A}+F^*+\mathfrak{L}^{-1}) \\ &\quad \times e^{-\hat{x}/\mathfrak{L}}+\mathrm{Ro}\hat{A}+F^*-\mathfrak{L}^{-1}]/[Ce^{-\hat{x}/\mathfrak{L}}+1] \\ \mathfrak{L} &\equiv [(\mathrm{Ro}\hat{A}+F^*)^2-4\hat{A}F^*\,\mathrm{Ro}\tilde{C}_D^2]^{-\frac{1}{2}} \\ C &\equiv -[2F^*\,\mathrm{Ro}\tilde{C}_D^2\hat{\zeta}(0)+\mathrm{Ro}\hat{A}+F^*-\mathfrak{L}^{-1}] \\ &\quad \div[2F^*\,\mathrm{Ro}\tilde{C}_D^2\hat{\zeta}(0)+\mathrm{Ro}\hat{A}+F^*+\mathfrak{L}^{-1}] \end{aligned}\right\} \quad (49)$$

In the case of zero upstream relative vorticity, the

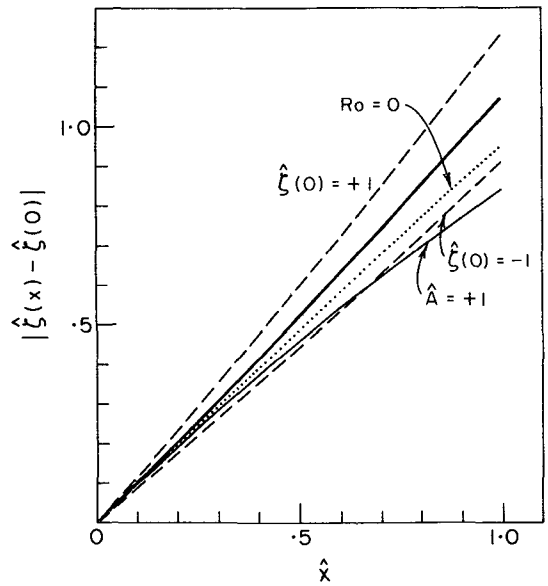

FIG. 4. Horizontal profiles of scaled relative vorticity magnitudes predicted by (49) for Ro=0.25, frictional parameter $F^*=0.1$, for downslope flow with zero initial vorticity (thick solid). Variations on this prototype are Ro=0 (dotted), upslope flow (thin solid), and positive and nonzero upstream vortices (dashed lines).

solution simplifies to

$$\hat{\zeta} = -(2\,\mathrm{Ro}F^*\tilde{C}_D{}^2)^{-1}(\mathrm{Ro}\hat{A}+F^*-\mathfrak{L}^{-1})(1-e^{-\hat{x}/\mathfrak{L}}) \div\{[-(\mathrm{Ro}\hat{A}+F^*-\mathfrak{L}^{-1})/(\mathrm{Ro}\hat{A}+F^*+\mathfrak{L}^{-1})]e^{-\hat{x}/\mathfrak{L}}+1\}. \quad (50)$$

The vorticity solutions (49) and (50) are evaluated for different values of Rossby number, frictional parameter F^* and initial vorticity in Figs. 4 and 5. To facilitate interpretation of the vorticity solution, we first temporarily consider an additional approximation. In general, the net acceleration-modification of the frictionally-induced vortex stretching is small as discussed previously and as is verified by evaluations of (50). It is then useful to form the ratio of the modification of $\mathfrak{L}^{-1}$ due to this particular frictional acceleration effect to $\mathfrak{L}^{-1}$ computed without this effect. This ratio is

$$P \equiv \frac{4F^*\mathrm{Ro}\tilde{C}_D{}^2\hat{A}}{(F^*+\mathrm{Ro}\hat{A})^2},$$

where P is expected to be generally much less than 1.[1]

[1] In the case of upslope flow, P will always remain less than 1 for possible atmospheric values of C_D and F^* and Rossby number small compared to 1. Thus, imaginary $\mathfrak{L}$, where the vorticity distribution becomes periodic with distance, is not of present interest. In fact, for $\mathrm{Ro}<\frac{1}{8}$, P remains less than 1 even as $\tilde{C}_D$ and/or F^* approach infinity. The most important exception to very small P is in downslope flow in the special case where $\mathrm{Ro}\hat{A}\approx -F^*$. Then the destruction of relative vorticity by boundary layer pumping is approximately balanced by the increased externally forced vorticity production associated with increased absolute vorticity in which case the quasi-geostrophic frictionless estimate is a good approximation.

We can then write

$$\mathfrak{L}^{-1} = (F^*+\mathrm{Ro}\hat{A})(1-(1/2)P),$$

where terms $O(P^2)$ have been neglected. The vorticity solution (50) then simplifies to

$$\hat{\zeta} \approx \frac{-\hat{A}}{\mathrm{Ro}\hat{A}+F^*}\left[\frac{1-\exp(-\hat{x}/\mathfrak{L})}{-[P/(4-P)]\exp(-\hat{x}/\mathfrak{L})+1}\right]. \quad (51)$$

The vorticity amplitude, toward which the vorticity is adjusting, $-\hat{A}(\mathrm{Ro}\hat{A}+F^*)^{-1}$, decreases with increasing frictional parameter; the adjustment rate $\mathfrak{L}^{-1}$, however, increases with increasing frictional parameter. These tendencies reflect the "damping" nature of boundary layer pumping. For small Ro and F^*, the vorticity at a given point decreases with increasing frictional parameter as can be seen by expanding the exponential terms in the vorticity solution (51) or by evaluating the complete vorticity solution (50) shown in Fig. 5.

The increase in vorticity production due to accelerations in downslope flow and the converse (evident in Fig. 4) can be estimated by expanding exponential terms in (51) for $\hat{x}/\mathfrak{L}\ll 1$ or can be most simply estimated for the case of no boundary layer pumping ($F^*=0$), in which case

$$\hat{\zeta} = -\mathrm{Ro}^{-1}(1-e^{-\hat{A}\,\mathrm{Ro}\hat{x}}) = -\hat{A}\hat{x}+\tfrac{1}{2}\mathrm{Ro}\hat{A}^2\hat{x}^2-O(\mathrm{Ro}^2\hat{A}^3\hat{x}^3). \quad (52)$$

The term $\frac{1}{2}\mathrm{Ro}\hat{A}^2\hat{x}^2$, which represents the approximate influence of relative vorticity on the externally forced

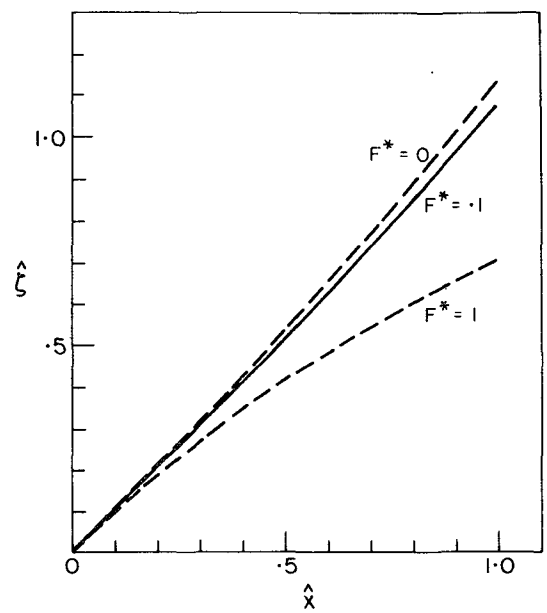

FIG. 5. Horizontal profiles of scaled relative vorticity predicted by Eq. (49) for Ro=0.2 for downslope flow with zero upstream relative vorticity for three different values of the frictional parameter F^*.

vortex stretching, increases vorticity production in downslope flow and vice versa.

Fig. 4 also illustrates the increase in vorticity production due to positive initial relative vorticity and vice versa. Since Ro is larger than F^*, in this example, the enhancement of vorticity production due to accelerations (positive relative vorticity) exceeds vorticity destruction due to increased boundary layer pumping.

b. Generalized forcing

In general for an arbitrary forcing distribution or terrain feature, the vorticity equation (48) cannot be solved analytically. Approximate solutions can be obtained by expanding the scaled relative vorticity in terms of the Rossby number. The zero- and first-order equations and solutions are

$$\left.\begin{aligned}
&\frac{\partial\hat{\zeta}_0}{\partial\hat{x}}=-F^*\hat{\zeta}_0-\hat{A}(\hat{x})\\
&\hat{\zeta}_0=e^{-F^*\hat{x}}\left[\hat{\zeta}_0(0)-\int_0^{\hat{x}}\hat{A}(\hat{x})e^{F^*\hat{x}}d\hat{x}\right]\\
&\frac{\partial\hat{\zeta}_1}{\partial\hat{x}}=-F^*\hat{\zeta}_1-\hat{A}(\hat{x})\hat{\zeta}_0-F^*\tilde{C}_D{}^2\hat{\zeta}_0{}^2\\
&\hat{\zeta}_1=e^{-F^*\hat{x}}\left[\hat{\zeta}_1(0)-\int_0^{\hat{x}}e^{F^*\hat{x}}\hat{A}(\hat{x})\hat{\zeta}_0(\hat{x})d\hat{x}\right.\\
&\qquad\left.-F^*\tilde{C}_D{}^2\int_0^{\hat{x}}e^{F^*\hat{x}}[\hat{\zeta}_0(\hat{x})]^2d\hat{x}\right]
\end{aligned}\right\},\quad(53)$$

where the subscript refers to the series expansion index.

To verify the usefulness of the series expansion solution (53), we estimate the solution for constant forcing from (53) for zero initial relative vorticity:

$$\hat{\zeta}_0+\mathrm{Ro}\hat{\zeta}_1=\frac{-\hat{A}}{F^*}\left\{(1-e^{-F^*\hat{x}})+\mathrm{Ro}\frac{\hat{A}}{F^*}[-(1-e^{-F^*\hat{x}})+(1-2\tilde{C}_D{}^2)F^*\hat{x}e^{-F^*\hat{x}}+\tilde{C}_D{}^2e^{-2F^*\hat{x}})]\right\}.\quad(54)$$

Comparison of evaluations of (54) for constant slope with the exact solution (50) indicates that for $F^*=0.1$ and $\mathrm{Ro}=0.25$, Eq. (54) incurrs a maximum error of only 1%.

As an example of generation of asymmetries in the vorticity distribution, we consider flow over a sinusoidal terrain feature with slope of the form

$$\hat{A}(\hat{x})=\pi\sin(2\pi\hat{x}),\quad 0\leqslant\hat{x}\leqslant 1,$$

in which case the zero-order vorticity amplitude with no boundary layer pumping is unity.

The vorticity solution obtained from (53) for the above symmetric forcing with zero initial vorticity is

$$\begin{aligned}
\hat{\zeta}(\hat{x})=&\pi F_1(-F^*\sin(k\hat{x})+k\cos(k\hat{x})-ke^{-F^*\hat{x}})\\
&-\mathrm{Ro}\pi^2F_1e^{-F^*\hat{x}}F^*\{(F_1F^{*2}\tilde{C}_D{}^2-1)\\
&\times F_3[(F^*\sin(k\hat{x})-2k\cos(k\hat{x})e^{F^*\hat{x}}\sin(k\hat{x})\\
&+(2k^2e^{F^*\hat{x}}/F^*)-2k^2/F^*]-F_2(1-\cos(k\hat{x}))\\
&+1/2kF_2F_3[e^{F^*\hat{x}}(F^*\sin(2k\hat{x})\\
&-2k\cos(2k\hat{x})+2k]+F_1k^2\tilde{C}_D{}^2\\
&\times[F^{*-1}(1-e^{-F^*\hat{x}})-2k^{-1}\sin(k\hat{x})\\
&+F_3(2F^{*-1}k^2e^{F^*\hat{x}}-2F^{*-1}k^2-F^*\\
&+e^{F^*\hat{x}}\cos(k\hat{x})(F^*\cos(k\hat{x})+2k\sin(k\hat{x})))]\},\quad(55)
\end{aligned}$$

where

$$\begin{aligned}
&F_1\equiv(F^{*2}+k^2)^{-1},\\
&F_2\equiv F^{*-1}-2F_1F^*\tilde{C}_D{}^2,\\
&F_3\equiv(F^{*2}+4k^2)^{-1},\\
&k\equiv 2\pi.
\end{aligned}$$

Fig. 6 shows evaluations of (55). The net production of relative vorticity is small for $F^*=0.1$ but somewhat larger for $F^*=1$ (large drag coefficient or thin free-flow depth). That is, asymmetries in the vorticity profile and net vorticity production are due to boundary layer pumping. Since potential vorticity is conserved for a homogeneous fluid, net vorticity changes over a symmetric terrain feature occur only when the boundary layer experiences a net change in depth (or acts as a net mass sink or source). As an example, net positive vorticity production across a symmetric terrain feature is evident in the laboratory experiments of Boyer (1971). The net production of nonzero relative vorticity associated with boundary layer pumping is small for typical atmospheric values of the external parameters as can be seen from evaluations of (55), shown in Fig. 6, or by integrating (48) for the case of flow over a symmetric ridge.

As a result of the destruction of anticyclonic vorticity by boundary layer pumping in flow over the above terrain feature, the maximum vorticity magnitude occurs upstream slightly from the forcing maximum (Fig. 6). The influence of accelerations (Fig. 6) is seen to reduce the vorticity production, a result of decreased absolute vorticity. However, the occurrence of nonzero accelerations does not generate a significant net vorticity change since the net change associated with accelerations is zero without boundary layer pumping and frictional-acceleration interactions are small.

7. Summary and further discussion

The above simple solutions illustrate the following flow tendencies partially predicted by scale analysis of synoptic-scale flow:

1) The penetration depth of the influence of boundary layer pumping or arbitrary forcing in the atmosphere is fL/N, where N is the Brunt-Väisälä frequency and L the horizontal length scale of the flow.

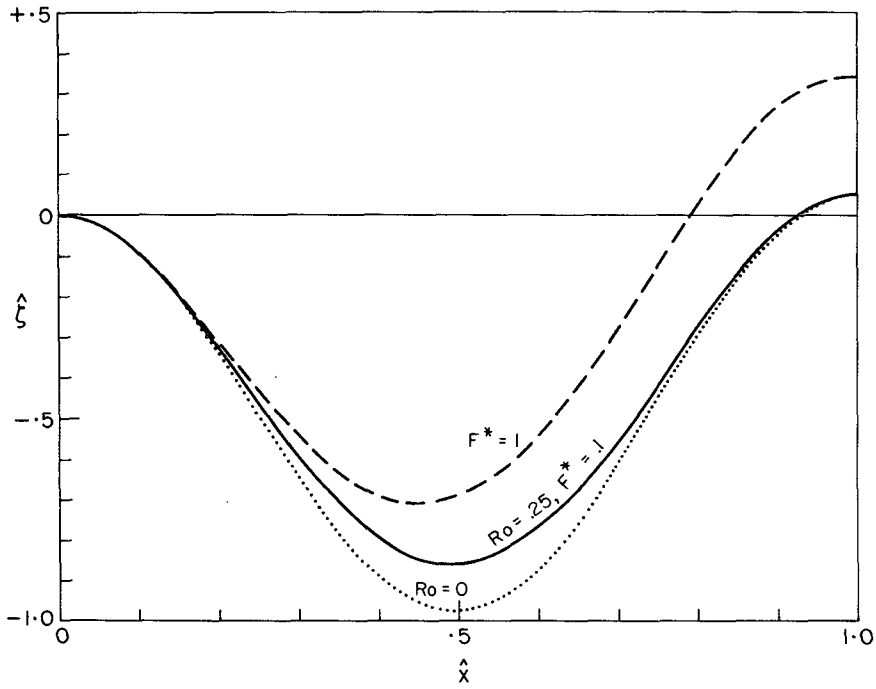

FIG. 6. Horizontal profiles of scaled relative vorticities over sinusoidal terrain predicted by (55) for zero upstream relative vorticity for Ro=0.25, F^*=0.1 (thick solid), Ro=0.25, F^*=1 (dashed) and Ro=0, F^*=0.1 (dotted).

2) The spin-down rate associated with boundary layer pumping is proportional to the surface stress and inversely proportional to the above free-flow depth scale. In particular, the spin-down time scale is $N^{-1}L/F$, where F is the boundary layer pumping efficiency (boundary layer pumping rate divided by the geostrophic vorticity). Calculations presented in this study indicate that boundary layer pumping may significantly alter the lower troposphere on a synoptic time scale with large surface stress and significant free-flow stratification. Boundary layer pumping appears to have a small direct synoptic scale influence on the middle and upper troposphere.

3) For slopes characteristic of the high plains of the United States and typical wintertime stratification, orographical forcing appears to be quite important from a climatic point of view.

4) Effects due to boundary layer pumping and free-flow accelerations oppose each other with cyclonic vorticity as is produced in downslope flow while such effects both act to retard vorticity production in regions of anticyclonic vorticity. Thus, for a given slope magnitude and zero upstream vorticity, vorticity production is greater in downslope flow while vertical motions are greater in upslope flow.

5) Due to near cancellation of already small effects from the influence of accelerations on the boundary layer pumping rate and the influence of free-flow accelerations on the vortex stretching due to a given boundary layer pumping rate, the net interaction between accelerations and boundary layer pumping is generally unimportant.

6) In flow over symmetric orography or external forcing, the net production of vorticity is small.

The above study also indicates the usefulness of examining atmospheric vorticity dynamics with isentropic coordinates. In such a coordinate system the stratification parameter varies slowly with elevation in the troposphere and tilting and vertical advection terms are implicitly included for adiabatic flow without complicating the mathematics.

The above theory is useful in predicting the possible importance of various effects and their qualitative behavior but cannot predict details of circulation development in the more complicated atmosphere where effects due to stratification in the boundary layer, diabatic heating, and interactions with sub-synoptic scales of motion are likely to be important. For example, developments in this study have addressed only the influence of synoptic-scale boundary layer pumping and have not considered mesoscale structure. In actual mid-latitude cyclones, much of the low-level rising motion is concentrated in frontal zones. In cloudless areas such as frequently occur behind the cold front or within the warm air mass, nighttime radiational cooling may lead to substantial stratification and baroclinity in the boundary layer, resulting in possible reduction of the frictionally driven circulation or resulting in local disruption due to drainage flows.

Acknowledgments. This research was supported by Research Grant DES 73-06540 A01, Atmospheric Sciences Section, National Science Foundation. We greatfully acknowledge the reviewers for important suggestions.

REFERENCES

Batchelor, G. K., 1970: *An Introduction to Fluid Dynamics*. Cambridge University Press, 615 pp.

Bleck, Rainer, 1973: Numerical forecasting experiments based on the conservation of potential vorticity on isentropic surfaces. *J. Appl. Meteor.*, **12**, 737–752.

Boyer, D. L., 1971: Rotating flow over long shallow ridges. *Geophys. Fluid Dyn.*, **2**, 165–184.

Buzyna, C., and G. Veronis, 1971: Spin-up of a stratified fluid: Theory and experiment. *J. Fluid Mech.*, **50**, 579–608.

Charney, J. G., and A. Eliassen, 1949: A numerical method of predicting the perturbations of the middle latitude westerlies. *Tellus*, **1**, 38–54.

——, and ——, 1964: On the growth of the hurricane depression. *J. Atmos. Sci.*, **21**, 68–75.

Gates, W. Lawrence, 1961: Static stability measures in the atmosphere. *J. Meteor.*, **18**, 526–533.

Graystone, P., 1962: The introduction of topographic and frictional effects in a baroclinic model. *Quart. J. Roy. Meteor. Soc.*, **88**, 256–270.

Greenspan, H. P., and L. N. Howard, 1963: On the time-dependent motion of a rotating fluid. *J. Fluid Mech.*, **17**, 385–404.

Haltiner, G. J., 1971: *Numerical Weather Prediction*. Wiley, 317 pp.

Hess, S. L., and H. Wagner, 1948: Atmospheric waves in the northwestern United States. *J. Meteor.*, **5**, 1–19.

Hogg, N., 1973: On the stratified Taylor column. *J. Fluid Mech.*, **58**, 517–537.

Holton, J. R., 1965: The influence of viscous boundary layers on transient motions in a stratified rotating fluid. Part I. *J. Atmos. Sci.*, **22**, 402–411.

——, 1975: On the influence of boundary layer friction on mixed Rossby-gravity waves. *Tellus*, **27**, 107–115.

Huppert, H. E., and M. E. Stern, 1974: The effect of sidewalls on homogeneous, rotating flow over two-dimensional obstacles. *J. Fluid Mech.*, **62**, 417–436.

Ingersoll, A. P., 1969: Inertial Taylor columns and Jupiter's Great Red Spot. *J. Atmos. Sci.*, **26**, 744–752.

Klemp, J. B., and D. K. Lilly, 1975: The dynamics of wave-induced downslope winds. *J. Atmos. Sci.*, **32**, 320–339.

Kuo, H. L., 1956: On quasi-nondivergent prognostic equations and their integration. *Tellus*, **8**, 373–383.

——, 1973: Planetary boundary layer flow of a stable atmosphere over the globe. *J. Atmos. Sci.*, **30**, 53–65.

Lilly, D. K., 1968: Models of cloud-topped mixed layers under a strong inversion. *Quart. J. Roy. Meteor. Soc.*, **94**, 292–309.

Mahrt, L., 1974: Time-dependent, integrated, planetary boundary layer flow. *J. Atmos. Sci.*, **31**, 457–464.

——, 1975: The influence of momentum advections on a well-mixed layer. *Quart. J. Roy. Meteor. Soc.*, **101**, 1–11.

McClain E. P., 1960: Some effects of the Western Cordillera of North America on cyclonic activity. *J. Meteor.*, **17**, 104–115.

Newton, C. W., 1956: Mechanism of circulation change during a lee cyclogenesis. *J. Meteor.*, **13**, 528–539.

Petterssen, S., 1956: *Weather Analysis and Forecasting*, 2d ed., Vol. I. McGraw–Hill, 428 pp.

Phillips, N. A., 1963: Geostrophic motion. *Rev. Geophys.*, **1**, 123–176.

Sakurai, T., 1969: Spin-down problem of rotating stratified fluid in thermally insulated circular cylinders. *J. Fluid Mech.*, **37**, 689–699.

Sawyer, J. S., 1959: The introduction of the effects of topography into methods of numerical forecasting. *Quart. J. Roy. Meteor. Soc.*, **85**, 31–34.

Thompson, P. D., 1961: *Numerical Weather Analysis and Prediction*. Macmillan, 170 pp.

U. S. Weather Bureau, 1957: Upper-air climatology of the United States. Tech. Paper No. 32, U. S. Weather Bureau, Washington, D. C., 199 pp.

Walin, G., 1969: Some aspects of time-dependent motion of a stratified rotating fluid. *J. Fluid Mech.*, **36**, 289–307.

Young, J. A., 1973: Isallobaric air flow in the planetary boundary layer. *J. Atmos. Sci.*, **30**, 1584–1592.